MFG-E8/Lactadherin Promotes Tumor Growth in an Angiogenesis-Dependent Transgenic Mouse Model of Multistage Carcinogenesis

Melanie Neutzner,[1] Theresa Lopez,[2] Xu Feng,[1] Elke S. Bergmann-Leitner,[3] Wolfgang W. Leitner,[1] and Mark C. Udey[1]

[1]Dermatology Branch and [2]Basic Research Laboratory, Center for Cancer Research, National Cancer Institute, NIH, Bethesda, Maryland and [3]Department of Immunology, Walter Reed Army Institute of Research, Silver Spring, Maryland

Abstract

The relevance of angiogenesis in tumor biology and as a therapeutic target is well established. MFG-E8 (also termed lactadherin) and developmental endothelial locus 1 (Del1) constitute a two-gene family of $\alpha_v\beta_3/\beta_5$ ligands that regulate angiogenesis. After detecting MFG-E8 mRNA in murine tumor cell lines, we sought to determine if MFG-E8 influenced tumorigenesis in Rip1-Tag2 transgenic mice, a cancer model in which angiogenesis is critical. MFG-E8 mRNA and protein were increased in angiogenic islets and tumors in Rip1-Tag2 mice compared with normal pancreas. Frequencies of angiogenic islets and tumor burdens were decreased in MFG-E8–deficient Rip1-Tag2 mice compared with those in control Rip1-Tag2 mice. Invasive carcinomas were modestly underrepresented in MFG-E8–deficient mice, but tumor frequencies and survivals were comparable in these two strains. Absence of MFG-E8 also led to decreases in tumor vascular permeability without obvious changes in vascular morphology. Decreased proliferation was noted in angiogenic islets and increases in apoptotic cells were detected in islets and tumors. Compensatory increases in mRNA encoding proangiogenic proteins, including FGF2, in angiogenic islets, and Del1, in angiogenic islets and tumors, were also detected in MFG-E8–deficient mice. MFG-E8 and its homologue Del1 may represent relevant targets in cancer and other diseases in which angiogenesis is prominent. [Cancer Res 2007;67(14):6777–85]

Introduction

Sustained angiogenesis is a prerequisite for solid tumor growth (1, 2), and the importance of this complex biological process as a target in cancer patients has been validated. Angiogenesis is regulated by both proangiogenic and antiangiogenic factors, and considerable redundancy exists. Proangiogenic proteins, including vascular endothelial growth factor (VEGF), acidic and basic fibroblast growth factors (FGF1 and FGF2), and members of the angiopoietin family, trigger signal transduction events that eventuate in increased endothelial cell proliferation, survival, and migration by engaging transmembrane receptor tyrosine kinases on endothelial cells.

There is considerable cross-talk between growth factor receptor–dependent and integrin-dependent signaling (3), and integrin-dependent signaling also regulates angiogenesis (4, 5). Indeed, $\alpha_v\beta_3$ integrin associates with VEGF receptor 2 (VEGFR2; ref. 6), and engagement of integrins can enhance endothelial cell survival and migration (7). VEGF also stimulates the expression of $\alpha_v\beta_3$ and $\alpha_v\beta_5$ integrins on angiogenic vasculature, thereby potentiating effects of VEGF receptor engagement. Recent studies in mice expressing a mutant form of β_3 integrin that is unable to undergo tyrosine phosphorylation confirmed the important role that this integrin plays in pathologic angiogenesis and provide important mechanistic insights (8).

Pharmacologic inhibitors of VEGF and FGF receptor kinases and antibodies that bind to these growth factors or their receptors have been extensively studied in animal models of cancer and clinical trials in cancer patients are under way. Emerging data indicate that treatment with anti-VEGF monoclonal antibody (mAb), in conjunction with other agents, can prolong patient survival but does not induce complete remissions. Indeed, development of resistance to antiangiogenic treatments has been observed in both murine and xenotransplantation models. In the Rip1-Tag2 transgenic mouse model of pancreatic cancer (see below), for example, inhibition of VEGFR2 receptor signaling with an inhibitory antibody initially stabilized disease. However, pancreatic tumors eventually progressed despite continuous treatment with the antibody due to the up-regulation of other proangiogenic factors (9). Thus, targeting multiple compensatory or complementary proangiogenic pathways may be required to achieve maximal therapeutic effects. Identification of new proteins or receptors that modulate angiogenesis in the setting of cancer may allow development of new antiangiogenic cancer therapy strategies that address this problem.

The importance of the $\alpha_v\beta_3/\beta_5$ ligands developmental endothelial locus 1 (Del1) and MFG-E8, a closely related homologue, as regulators of angiogenesis has recently been recognized. Del1 was initially identified as a locus that was selectively active in endothelial cells in mouse embryos (10, 11). Del1 protein promotes $\alpha_v\beta_3$-dependent endothelial cell attachment and migration as well as integrin clustering and the formation of focal contacts (12). Subsequent studies showed that Del1 derives from several extraembryonic sources, including subpopulations of murine phagocytes and a variety of human cancer cell lines. In a xenotransplantation model, overexpression of Del1 accelerated tumor growth in association with increased vascular density and decreased tumor cell apoptosis (13). Del1 also promoted vascularization of ischemic muscle and exhibits proangiogenic activity in the chicken chorioallantoic membrane assay (14).

Del1 shares both structural and functional homology with MFG-E8, a 51-kDa secreted glycoprotein that was initially described in association with milk fat globules (15). Structurally, MFG-E8 is composed of two epidermal growth factor (EGF)-like domains at the NH_2 terminus and two discoidin-like and factor

Note: Supplementary data for this article are available at Cancer Research Online (http://cancerres.aacrjournals.org/).

M. Neutzner and T. Lopez are co–first authors.

Requests for reprints: Mark C. Udey, Dermatology Branch, Center for Cancer Research, National Cancer Institute, NIH, Building 10, Room 12N238, Bethesda, MD 20892-1908. Phone: 301-496-2481; Fax: 301-496-5370; E-mail: udey@helix.nih.gov.

doi:10.1158/0008-5472.CAN-07-0165

V/factor VIII–like domains (C1 and C2) at the COOH terminus. The second EGF-like domain contains an arginine-glycine-aspartic acid (RGD) motif, and this region of the protein binds to $\alpha_v\beta_3$ and $\alpha_v\beta_5$ integrins. The C2 domain has affinity for negatively charged and oxidized phospholipids, including phosphatidylserine, which is exposed on the surfaces of early apoptotic cells (16). By acting as a bridging molecule between apoptotic cells and phagocytes, MFG-E8 opsonizes apoptotic cells for clearance by phagocytes via an $\alpha_v\beta_3/\beta_5$-dependent mechanism (17). Like other mice that exhibit defective apoptotic cell clearance, MFG-E8–deficient mice develop an autoimmune phenotype that is characterized by autoantibody production, splenomegaly, and histologic evidence of glomerulonephritis (18). In a mouse model of acute hind limb ischemia, MFG-E8 also enhanced revascularization and promoted VEGF-induced Akt phosphorylation and endothelial cell survival in an integrin $\alpha_v\beta_3$- and $\alpha_v\beta_5$-dependent manner (19).

We documented expression of MFG-E8 in a variety of mouse cancer cell lines and hypothesized that MFG-E8 might promote tumorigenesis. To test this hypothesis, we crossed mice that were MFG-E8 deficient with Rip1-Tag2 mice. Rip1-Tag2 mice represent a well-characterized transgenic model of multistage carcinogenesis in which expression of the SV40 large T antigen is directed to the insulin-producing β cells of the pancreas by the rat insulin promoter (20). Pancreatic islets are morphologically normal until 4 to 6 weeks of age when a subset of islets becomes hyperproliferative and subsequently acquires an angiogenic phenotype (21) characterized by formation of dilated, leaky vessels. This process has been termed the "angiogenic switch." A subset of angiogenic islets develops into adenomas and invasive carcinomas (22).

Matrix metalloproteinase-9 (MMP-9) triggers the angiogenic switch by generating soluble truncated VEGF-A isoforms, thereby increasing the bioavailability and activity of this critical growth factor (23). Genetic ablation of MMP-9 or VEGF-A, or inhibition of the activities of these proteins by pharmacologic agents or antibodies, severely compromises tumor vascularization and initial tumor growth (9, 23–26). Conversely, overexpression of VEGF-A in islet cells enhances angiogenesis and tumorigenicity (27). Because tumor development in Rip1-Tag2 mice is dependent on VEGF-induced angiogenesis, we used this model in conjunction with MFG-E8–deficient mice that we generated to assess the involvement of MFG-E8 in tumorigenesis. Herein, we document that MFG-E8 plays a nonredundant role as a promoter of tumor-related angiogenesis and tumor growth in an important *in vivo* model of neoplasia.

Materials and Methods

Mice. Transgenic Rip1-Tag2 mice (20) were obtained from the National Cancer Institute (NCI) Mouse Models for Human Cancers Consortium. MFG-E8 knockout (KO) mice were generated by replacing exons 2 to 6 of the gene encoding MFG-E8 in 129SvJ ES cells with a neomycin resistance cassette. Heterozygous founders were speed backcrossed to C57BL/6NCr mice to generate animals with appropriate and uniform genetic backgrounds. MFG-E8–deficient mice were generated by interbreeding heterozygous animals carrying the KO allele. Female MFG-E8$^{-/-}$ mice were mated with male Rip1-Tag2 mice and male progeny carrying the Rip1-Tag2 transgene and the mutant MFG-E8 allele were crossed with female MFG-E8$^{-/-}$ mice to generate animals of interest. Mice were genotyped by PCR using the following primers: Rip1-Tag2, GGACAAACCACAACTAGAATGCAGTG (forward) and CAGAGCAGAATTGTGGAGTGG (reverse); Neo, GCCAGAGGCCACTTGTGTAG; and MFG-E8, CTCTCAGATTCACCTGCTCGTG and CACCGTTCAGGCACAGGCTG. Animals were housed and used in experiments in accordance with institutional guidelines.

Cell lines. B16.F10 (Tumor Repository of the NCI/Frederick Cancer Research and Development Center, Frederick, MD), LLC (generous gift from Kevin Camphausen, NCI, Bethesda, MD), TC-1 (generous gift from T.C. Wu, Johns Hopkins University, Baltimore, MD), RMA (generous gift from Jon Yewdell, National Institute of Allergy and Infectious Diseases, Bethesda, MD), and MB49 (generous gift from Terry Fry, NCI) cells were maintained in RPMI 1640 with 10% fetal bovine serum (FBS). Pancreatic tumor cell lines were isolated as described previously (28), characterized by staining for SV40 large T antigen, and maintained in DMEM with 15% FBS.

Enumeration of angiogenic islets and determination of tumor burden. Angiogenic islets were prepared from pancreata that had been perfused with collagenase IV solution in a retrograde fashion (29). Islets were recovered from partially digested tissue using a stereomicroscope and scored as angiogenic when they displayed red surface patches. In other experiments, tumors were isolated from nondigested tissue by microdissection and measured in two perpendicular dimensions. Tumor volumes were calculated in accordance with the following formula: volume = length × width^2 × 0.52.

Immunofluorescence. Immunofluorescence staining was done on 8-μm frozen tissue sections. Sections were fixed with cold acetone and blocked for nonspecific antibody binding with TNB buffer (Perkin-Elmer) supplemented with 5% normal donkey serum and for nonspecific biotin binding with streptavidin/biotin blocking kit (Vector Laboratories). After inactivation of endogenous peroxidases with 3% H_2O_2 (15 min at room temperature), digoxigenin-conjugated mouse anti-mouse anti-MFG-E8 mAb generated in our laboratory (1H6) was added (1 μg/mL). Tissue-bound anti-MFG-E8 was detected after serial incubations with anti-digoxigenin-horseradish peroxidase (HRP)-coupled secondary antibody (0.75 unit/mL; Roche), biotin-tyramide (1:50; Perkin-Elmer), and finally Alexa Fluor 546-streptavidin (5 μg/mL; Molecular Probes). Endothelial cells were stained with a rat anti-CD31 mAb (clone MEC13.3, 0.15 μg/mL; BD PharMingen) followed by donkey anti-rat Cy2-labeled secondary antibody (6 μg/mL; Jackson ImmunoResearch). Pericytes were stained with a rabbit anti-NG2 (5 μg/mL; Chemicon) polyclonal antibody followed by donkey anti-rabbit Cy2-labeled secondary antibody (12 μg/mL; Jackson ImmunoResearch). Leucocytes and macrophages were stained with rat anti-CD45 (clone IBL-3/16, 20 μg/mL; Serotec) or rat anti-CD68 (clone FA-11, 5 μg/mL; Serotec) followed by donkey anti-rat Cy2 secondary antibody. Sections were counterstained with 4′,6-diamidino-2-phenylindole (DAPI) to visualize nuclei, mounted in Fluoromount-G (Electron Microscopy Sciences), and studied using an Axio Imager A1 microscope. Images were captured using an AxioCam MRm camera and Axio Vision software 4.5 (Zeiss) and processed with Adobe Photoshop before presentation.

Assessment of vascular permeability. Vessel permeability was assessed by determining the amount of tissue-extravasated dye after i.v. injection [Miles assay (30)]. Mice were injected with Evans blue dye (1% stock; Sigma) at a dose of 30 mg/kg body weight. After 30 min, animals were euthanized and perfused with 10 mL of 1% paraformaldehyde in 0.05 mol/L citrate buffer (pH 3.4). Pancreata and spleens were removed and tumors were recovered by dissection. After incubation in formamide for 18 h at 55°C, retained (extravasated) dye was quantified using spectrophotometry by determining absorbance at 610 nm and normalized to sample weights. Permeability of pancreatic tumor vessels is expressed relative to permeability of normal splenic vessels (each value determined in individual animals).

Visualization of vessels. To allow visualization of blood vessels in tumors and normal tissue, anesthetized mice were injected via tail veins with 0.1 mg FITC-labeled *Lycopersicon esculentum* lectin (1 mg/mL in saline; Vector Laboratories). After 3 min, mice were heart perfused with 10 mL of 4% paraformaldehyde in PBS. Pancreatic tissue was excised, frozen in OCT, and stored at −80°C. Frozen sections (40 μm) were prepared, counterstained with DAPI, mounted, and visualized under fluorescent light with an Axio Imager A1 microscope with an AxioCam MRm camera and Axio Vision 4.5 software.

Measurement of proliferation *in situ*. Mice were injected i.p. with 100 μg/g body weight of bromodeoxyuridine (BrdUrd; 10 mg/mL in water;

Sigma) and euthanized 2 h later. Pancreata were harvested, fixed overnight in 4% paraformaldehyde, and embedded in paraffin. Sections (5 μm) were deparaffinized and rehydrated, and antigen retrieval was done by incubation in citrate buffer (Chemicon) for 20 min at 94°C followed by 20 min at room temperature. To visualize BrdUrd via light microscopy, sections were incubated with mouse anti-BrdUrd mAb (Bromo-2′-deoxyuridine Labeling and Detection Kit II, Roche). Anti-BrdUrd mAb was detected with a biotinylated anti-mouse antibody (1:250 MOM kit, Vector Laboratories) in conjunction with Vectastain R.T.U. ABC peroxidase complex (Vector Laboratories). Sections were developed with NovaRed peroxidase substrate (Vector Laboratories), counterstained with hematoxylin, and mounted in aqueous mounting medium. For quantification, graded lesions were counted in a blinded fashion (three mice per group) using light microscopy (Leica DMIRB microscope equipped with Retiga 1300 camera and OpenLab 3.1.7 software, Improvision).

Measurement of apoptotic indices. Apoptotic cells were identified by terminal deoxynucleotidyl transferase (TdT)-mediated dUTP nick end labeling (TUNEL) using an *in situ* cell death detection kit (Roche). Formalin-fixed, paraffin-embedded tissue sections (5 μm) were deparaffinized and rehydrated. After treatment with proteinase K (Dako) for 5 min, DNA strand breaks were labeled by TdT (diluted 1:10 in TUNEL dilution buffer; Roche) with FITC-conjugated nucleotides. FITC label was revealed by a HRP-conjugated anti-FITC antibody and NovaRed substrate. Sections were counterstained with hematoxylin before visualization of apoptotic and normal nuclei in graded lesions using light microscopy (see above). For quantification, lesions were counted in a blinded fashion (four mice per group).

RNA isolation and reverse transcription-PCR. Total RNA was isolated with RNeasy kits (Qiagen) according to the manufacturer's recommendation after homogenizing tissue with a Mixer Mill MM200 (Retsch) for 4 min at 20 Hz. Reverse transcription was accomplished with SuperScript III kits (Invitrogen). Qualitative PCR was done for MFG-E8 (forward, 5′-ATCTACTGCCTCTGCCCTGA-3′; reverse, 5′-ACACATACGAGGCGGAAATC-3′) and actin (forward, 5′-TGTGATGGTGGGAATGGGTCAG-3′; reverse, 5′-TTTGATGTCACGCACGATTTCC-3′). Real-time reverse transcription-PCR (RT-PCR) was done using commercially available primers and probes from Applied Biosystems and an ABI Prism 7000 sequence detection instrument (Applied Biosystems) equipped with ABI Prism 7000 SDS software version 1.0.

Statistical analysis. All statistical analysis was done by use of the Mann-Whitney test. Error bars in figures represent SE. P values of <0.05 were considered statistically significant.

Results

Expression and localization of MFG-E8 during tumorigenesis in Rip1-Tag2 mice. RT-PCR analysis revealed MFG-E8 mRNA expression in multiple murine cancer cell lines from melanomas and lung and bladder carcinomas as well as a T-cell lymphoma line (Fig. 1*A*) and cell lines established from tumors in Rip1-Tag2 mice (Fig. 1*B*). To determine if this known proangiogenic protein might play a role in tumorigenesis *in vivo*, we assessed MFG-E8 expression in a mouse model of angiogenesis-dependent neoplasia. Qualitative RT-PCR showed MFG-E8 mRNA expression in both angiogenic islets and tumors from Rip1-Tag2 mice (Fig. 1*C*). Under these conditions, MFG-E8 mRNA was not detected in normal pancreas nor in islets or tumors isolated from Rip1-Tag2 MFG-E8 KO animals. In an attempt to quantify relative amounts of MFG-E8 in tumors and precursor lesions, we did quantitative RT-PCR with Taqman probes. Although data from these experiments indicated that MFG-E8 message was ~3-fold more abundant in angiogenic islets than in tumors, different procedures were used to prepare the samples, by necessity, and definitive conclusions are therefore not possible. Del1, an MFG-E8 homologue that was previously implicated in tumorigenesis, was also expressed at the mRNA level in angiogenic islets and tumors but not in normal pancreatic tissue (data not shown).

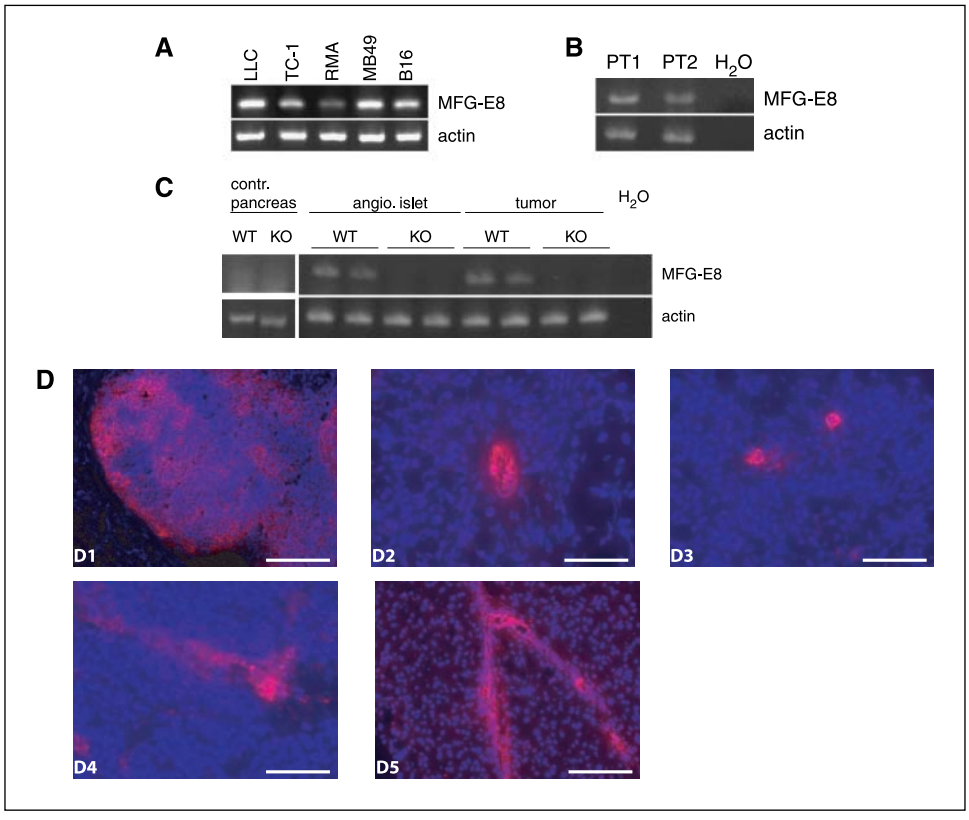

Figure 1. Expression of MFG-E8 in cancer cell lines and during islet cell tumorigenesis. *A,* MFG-E8 expression assessed by RT-PCR in murine cancer cell lines. *Lane 1,* Lewis lung carcinoma cells; *lane 2,* TC-1 lung cancer cells; *lane 3,* RMA T-cell lymphoma; *lane 4,* MB49 bladder carcinoma; *lane 5,* B16 melanoma. *B,* RT-PCR of MFG-E8 in two independently isolated pancreatic tumor cell lines (PT1 and PT2). *C,* detection of MFG-E8 mRNA in WT pancreas and in angiogenic islets and tumors from Rip1-Tag2 mice and Rip1-Tag2 mice deficient for MFG-E8 using RT-PCR. *D,* distribution of anti-MFG-E8 immunoreactivity in tumors (*D2–D4*) in Rip1-Tag2 mice and in exocrine pancreas (*D5*) and lymph node (*D1*). Bars, 50 μm (*D2–D4*) and 100 μm (*D1* and *D5*).

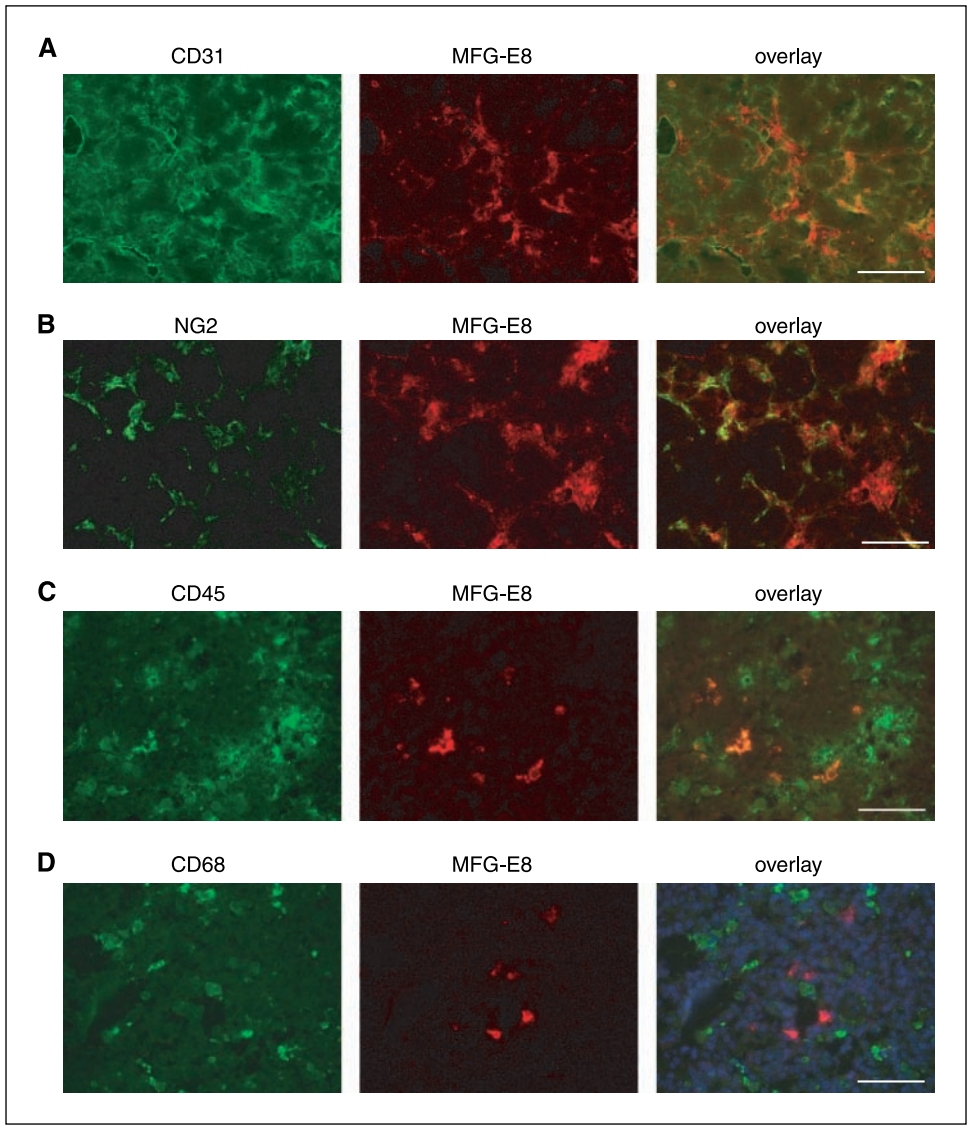

Figure 2. Localization of MFG-E8 in pancreatic tumors in Rip1-Tag2 mice. *A,* immunofluorescence staining for the endothelial cell marker CD31 (*green*) and MFG-E8 (*red*) and overlay in a pancreatic tumor. Bar, 200 μm. *B,* immunofluorescence staining for the pericyte marker NG2 (*green*) and MFG-E8 (*red*) and overlay. Bar, 100 μm. *C,* immunofluorescence staining for the leukocyte marker CD45 (*green*) and MFG-E8 (*red*) and overlay. Bar, 50 μm. *D,* immunofluorescence staining for the macrophage marker CD68 (*green*) and MFG-E8 (*red*) and overlay. Bar, 50 μm.

MFG-E8 protein was localized in pancreatic tissue with a mouse anti-MFG-E8 mAb (1H6) that was generated by immunizing MFG-E8$^{-/-}$ mice with cDNA encoding full-length MFG-E8 protein.[4] Specificity of staining was assured by comparing staining patterns in MFG-E8–competent and MFG-E8–deficient mice as well as by comparing staining with previously published staining for MFG-E8 (Supplementary Fig. S1; ref. 18). Staining of intrapancreatic lymph nodes revealed accumulation of MFG-E8 protein in focal areas corresponding to germinal centers (Fig. 1*D1*) and in association with some CD68-positive macrophages as expected (18). Three distinct patterns of MFG-E8 staining were evident in pancreatic lesions in Rip1-Tag2 mice. Accumulation of MFG-E8 in proximity to CD31-positive blood vessels was the most obvious and frequent of the observed patterns (Figs. 1*D2* and 2*A*). Anti-MFG-E8 staining also accumulated in close proximity to perivascular cells that expressed the pericyte marker NG2 (Fig. 2*B*). Perhaps because MFG-E8 is a secreted protein, it was not possible to definitively determine if it was produced by endothelial cells, pericytes, or both cell types. Less frequently, MFG-E8 immunoreactivity was observed in association with single, or small groups of, cells (Fig. 1*D3*). These cells were identified as CD45-positive leukocytes that did not express the macrophage marker CD68 (Figs. 1*D3* and 2*C* and *D*). Finally, in some areas, MFG-E8 was distributed more diffusely (Fig. 1*D4*). Interestingly, although MFG-E8 mRNA was not readily detected in normal pancreas, MFG-E8 protein was identified in association with vessels in exocrine pancreas in control as well as Rip1-Tag2 mice (Fig. 1*D5*).

Involvement of MFG-E8 in the angiogenic switch and tumor growth. To assess the involvement of MFG-E8 in tumorigenesis *in vivo*, we generated MFG-E8 KO mice by replacing exons 2 to 6 with a neomycin cassette. As described previously (18, 19, 31), MFG-E8 KO mice are viable. Our C57BL/6 MFG-E8 KO animals did not exhibit obvious fertility defects and females were able to nurse multiple litters. Older MFG-E8–deficient mice exhibited splenomegaly, as previously reported (18), and autoantibodies were also detected. Importantly, histologic sections of pancreas from control and MFG-E8$^{-/-}$ mice were indistinguishable (data not shown).

[4] In preparation.

To address a possible role for MFG-E8 in the angiogenic switch, angiogenic islets were isolated from 10.5-week-old Rip1-Tag2 control animals as well as Rip1-Tag2 age- and sex-matched MFG-E8 KO mice. MFG-E8–deficient mice exhibited a 35% (P = 0.03) decrease in the number of angiogenic islets compared with control animals (Fig. 3*A*). KO animals also displayed a ~2-fold decrease in aggregate tumor burden at 12 (P = 0.007) and 13.5 (P = 0.01) weeks of age (Fig. 3*B*). This effect was attributable to decreased sizes of individual tumors, as the numbers of tumors per animal in both groups were similar (Fig. 3*C*). Histologic analysis using previously published staging criteria (32) revealed differences in tumor invasiveness between control and MFG-E8 KO animals characterized by an increase in adenomas and a decrease in invasive type 2 tumors in the absence of MFG-E8 (Fig. 3*D*). Intrapancreatic lymph node metastases developed in both groups with similar frequencies (data not shown), and survivals of sex-matched control and MFG-E8$^{-/-}$ Rip1-Tag2 mice were also comparable (data not shown). Together, these data indicate that MFG-E8 is critically involved in the angiogenic switch in pancreatic tumorigenesis but that it is not essential for progression of angiogenic islets to solid tumors.

Characterization of tumor vessels in MFG-E8–deficient Rip1-Tag2 mice. Enhanced activity of VEGF in angiogenic islets and tumors in Rip1-Tag2 mice results in tumor vessels that are dilated, tortuous, and leaky (23). The observation that MFG-E8 potentiates VEGF-dependent signaling (19) in conjunction with the perivascular location of MFG-E8 in angiogenic islets and tumors prompted us to characterize vessels in tumors in MFG-E8–deficient Rip1-Tag2 mice. Vascular permeability was assessed using the Miles assay. In comparison with control Rip1-Tag2 mice, permeability in tumor vessels in MFG-E8 KO mice was reduced by ~20% (Fig. 4*A*). However, pancreatic vascular structure in Rip1-Tag2 control and MFG-E8–deficient mice was indistinguishable after intravital i.v. administration of FITC-labeled tomato lectin (Fig. 4*B*).

Influence of MFG-E8 on proliferation and apoptosis during tumorigenesis in Rip1-Tag2 mice. MFG-E8 KO animals displayed ~50% reductions in cumulative tumor burden at both time points examined (Fig. 3*B*). Because tumor burden represents the net result of cell proliferation and cell death, we examined both variables in tumors and premalignant lesions in Rip1-Tag2 mice. Tumor cell proliferation was evaluated by labeling cells with BrdUrd *in situ* (Fig. 4*C*). Percentages of proliferating cells in control and MFG-E8 KO hyperplastic islets and tumors were indistinguishable. However, proliferation in angiogenic islets from MFG-E8 KO animals was decreased by ~25% compared with control angiogenic islets (P < 0.002).

Accumulation of apoptotic cells in Rip1-Tag2 pancreatic tissue was assessed by TUNEL staining. As shown in Fig. 4*D*, apoptotic cells were detectable even in normal islets. The number of TUNEL-positive cells was increased over baseline in both hyperplastic and angiogenic islets in control mice. Percentages of apoptotic cells in hyperplastic and angiogenic islets in MFG-E8 KO mice were additionally increased compared with those in control Rip1-Tag2 mice. Interestingly, apoptotic cells were less frequent in adenomas in MFG-E8–deficient mice than in hyperplastic and angiogenic islets and invasive carcinomas in the same animals, and frequencies of apoptotic cells in adenomas from control and MFG-E8

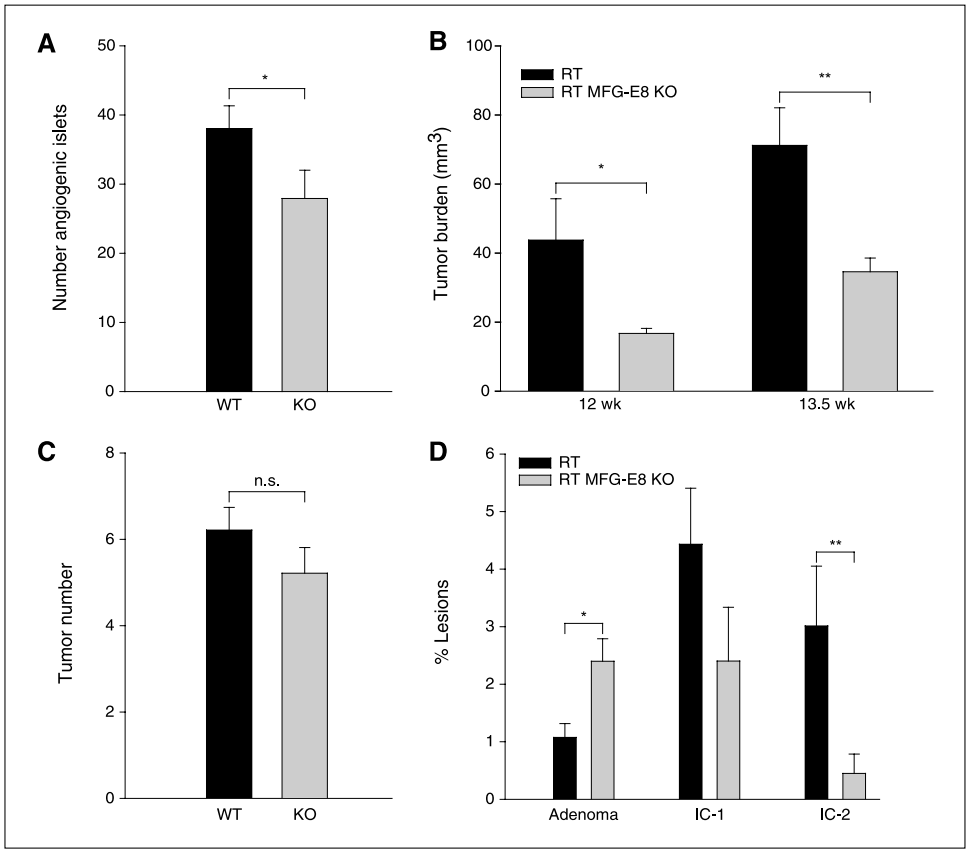

Figure 3. Importance of MFG-E8 in the angiogenic switch and tumor growth in Rip1-Tag2 mice. *A,* quantification of angiogenic islets (per mouse) in control (n = 9) and MFG-E8 KO (n = 10) Rip1-Tag2 mice. Angiogenic islets were isolated after retrograde pancreatic perfusion of 10.5-week-old mice with collagenase. *, P = 0.035. *B,* aggregate tumor burdens per mouse are depicted for control and MFG-E8 KO Rip1-Tag2 mice at 12 (n = 14) and 13.5 (n = 12–13) wks of age. *, P = 0.007; **, P = 0.01. *C,* tumors were recovered from 12-week-old control and MFG-E8 KO Rip1-Tag2 mice by microdissection and enumerated. Data are expressed as tumor number per mouse. *n.s.,* not significant. *D,* histologic staging of lesions in H&E-stained sections of pancreatic tissue from 13.5-week-old Rip1-Tag2 mice (n = 7). *, P < 0.05; **, P < 0.01.

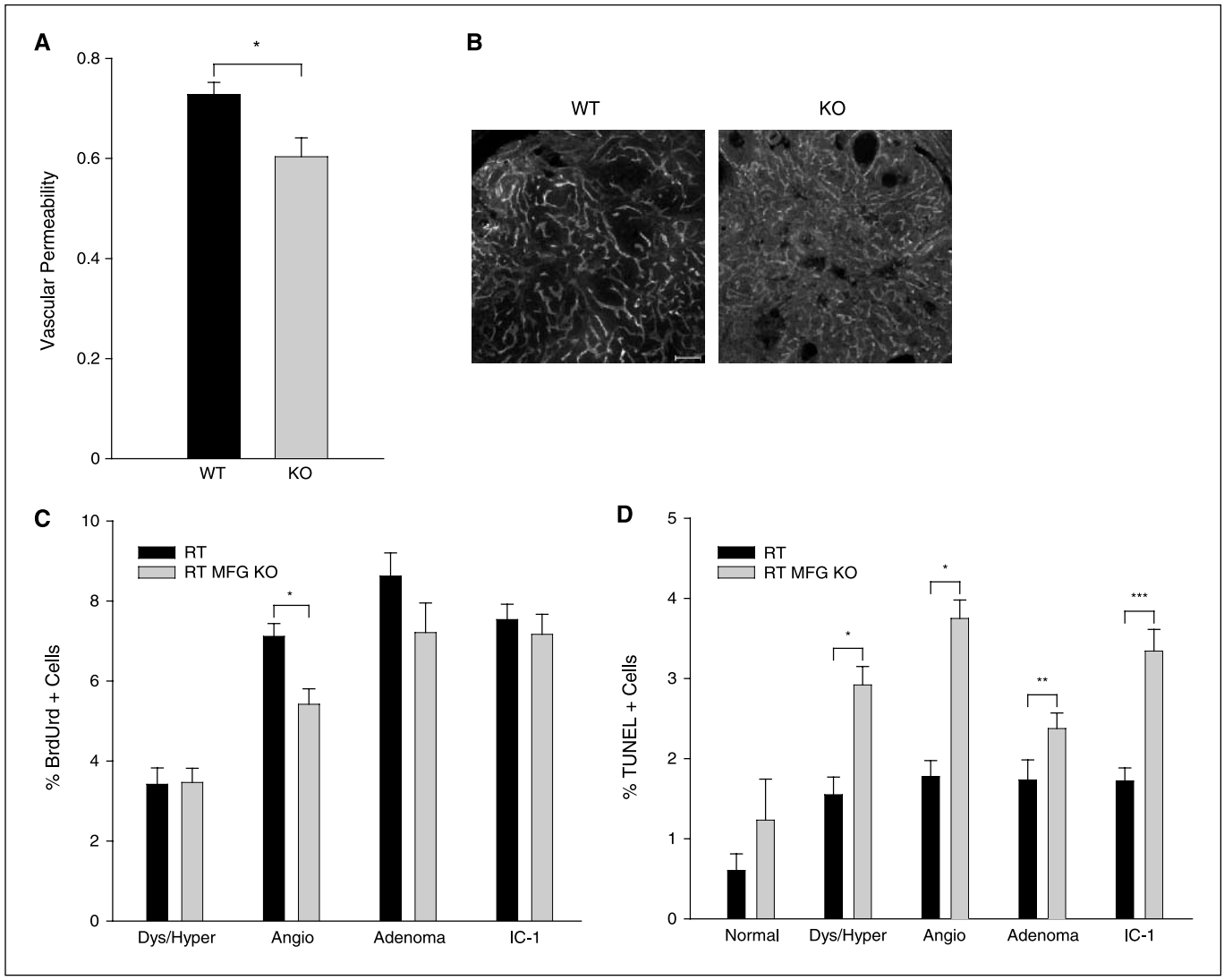

Figure 4. Influence of MFG-E8 on tumor vasculature, proliferation, and apoptosis. *A,* vascular permeability was quantified in control Rip1-Tag2 (n = 7) and MFG-E8 KO mice (n = 6) using the Miles assay. Extravasation of Evan's blue dye in pancreatic tumors (per unit weight) is expressed relative to dye extravasation in the spleens of the same animals (P < 0.05). *B,* visualization of vessel structure in tumors in control and MFG-E8$^{-/-}$ mice. Twelve-week-old mice were injected i.v. with FITC-*Lycopersicon esculentum* lectin and tumors were fixed *in situ*. Vessels were subsequently visualized in tissue sections using epifluorescence microscopy. Bar, 100 μm. *C,* quantification of proliferating cells by BrdUrd labeling. Proliferation in angiogenic islets in MFG-E8 KO mice was reduced relative to controls (P < 0.002). *D,* enhanced accumulation of apoptotic cells in islets at different stages of islet cell tumorigenesis as assessed by TUNEL staining. *, P < 0.0001; **, P = 0.08; ***, P < 0.002.

KO mice were not different from each other (P = 0.08). MFG-E8$^{-/-}$ animals did exhibit ~2-fold increases in percentages of TUNEL-positive cells in microinvasive carcinomas (P < 0.002), however. Because MFG-E8 enhances uptake of apoptotic cells by phagocytes, the observed increases in TUNEL-positive cells in pancreatic lesions in MFG-E8–deficient mice could reflect impaired clearance of apoptotic cells and/or increased apoptotic cell death. Attempts to quantify apoptotic cell death more directly via enumeration of early apoptotic cells were inconclusive because absolute numbers of active caspase-3–positive cells in islets and tumors were very low in both groups (data not shown).

Taken together, these results suggest that MFG-E8 promotes proliferation in premalignant angiogenic islets and may enhance cell survival as well. Although the reductions in BrdUrd labeling indices measured in MFG-E8$^{-/-}$ angiogenic islets were modest, the magnitudes of the differences are sufficient to explain the smaller cumulative pancreatic tumor burdens in Rip1-Tag2 MFG-E8 KO mice.

Compensation for MFG-E8 deficiency by up-regulation of proangiogenic regulators in Rip1-Tag2 pancreas. Acquisition of treatment resistance via compensatory increases in alternative proangiogenic mechanisms has been reported in RIP1-Tag2 mice after chronic administration of anti-VEGFR2 antibody (9). In this study, acute inhibition of VEGFR2 function caused hypoxia, which in turn led to up-regulation of angiogenic factors that do not signal through the VEGFR2 receptor (including FGF2). Thus, we sought to determine if loss of MFG-E8 function caused hypoxia or triggered changes in expression of angiogenic factors in lesions in Rip1-Tag2 pancreas. Staining for pimidazole adducts did not reveal chronic hypoxic conditions in tumors of MFG-E8 KO mice (data not shown).

To determine if compensatory proangiogenic mechanisms had been induced, we did real-time RT-PCR analysis on samples from

wild-type (WT) and MFG-E8 KO animals using a candidate approach to assess levels of expression of mRNAs encoding a variety of proteins that regulate angiogenesis. Expression of the MFG-E8 homologue Del1 was modestly increased in angiogenic islets of KO mice compared with angiogenic islets of WT mice and more strikingly up-regulated (1.8-fold) in tumors from KO mice (Fig. 5*A*). Although not definitive, these data suggest that compensatory up-regulation of Del1 in angiogenic islets and in tumors from MFG-E8–deficient mice may provide a partial explanation for the attenuated phenotype that we observed.

More extensive comparisons of gene expression profiles revealed additional modest differences in angiogenic islets from MFG-E8–deficient animals compared with controls (Fig. 5*B*). The most prominent change observed was in the expression of basic fibroblast growth factor (bFGF or FGF2), which showed a 2-fold increase in expression (Fig. 5*B*). VEGFR2, EphrinA2, and angiopoietin 2 mRNA levels were also somewhat increased in the absence of MFG-E8. Interestingly, assessment of proangiogenic factor gene expression levels in tumors from MFG-E8$^{-/-}$ mice revealed new patterns (Fig. 5*C*). FGF2 and VEGFR2 mRNAs, which were up-regulated in MFG-E8–deficient angiogenic islets, were equivalent in MFG-E8–deficient and control tumors. In contrast, levels of VEGF and EphrinA1 mRNA, which were comparable in angiogenic islets in the two strains, were modestly increased in MFG-E8$^{-/-}$ tumors. These results support the concept that MFG-E8 is an important factor in Rip1-Tag2 tumorigenesis and also suggest that different proangiogenic factors are critical in the early compared with late stages of tumor development.

Discussion

The present study documents that the proangiogenic secreted protein MFG-E8 promotes tumorigenesis in Rip1-Tag2 transgenic mice. MFG-E8 mRNA was easily detected in pancreatic tumors and in cell lines derived from these tumors but was not readily identified in normal pancreas. Localization of MFG-E8 protein in Rip1-Tag2 tumors revealed three distinctive patterns. Perivascular accumulation was the most frequent and most striking pattern noted. However, MFG-E8 was also found in a diffuse extracellular distribution as well as in association with single cells. The precise identity of these cells is uncertain, but MFG-E8–expressing cells are leukocytes that do not correspond to CD68-positive tumor-associated macrophages. Although pancreatic tumor cells produce MFG-E8 mRNA *in vitro*, we did not detect MFG-E8 protein in tumor cells *in situ* using immunohistochemistry. This suggests that MFG-E8 protein does not accumulate in the cells that produce it but rather that it accumulates in tissues that express relevant ligands.

Rip1-Tag2 MFG-E8–deficient mice exhibited aggregate tumor burdens that were ~2-fold lower than those in corresponding control mice. Frequencies of angiogenic islets in Rip1-Tag2 MFG-E8$^{-/-}$ mice were also ~35% lower than those in Rip1-Tag2 WT mice, and vascular permeability was reduced by ~20% in pancreatic tumors from MFG-E8–deficient mice. Tumor vessel frequencies and structure were not obviously different in MFG-E8$^{-/-}$ and WT mice, however. Absence of MFG-E8 also led to an ~25% decrease in proliferation of cells in angiogenic islets in MFG-E8 KO mice, although apoptotic cells were more frequent in several of the lesions (hyperplastic/dysplastic islets, angiogenic islets, and invasive carcinomas). The reduction in angiogenic precursor lesions that we observed in MFG-E8 KO mice did not result in decreased numbers of identifiable tumors. Although somewhat surprising, lack of concordance between angiogenic islet and tumor frequencies has been previously reported. In a β-cell–specific VEGF-A KO mouse, Inoue et al. (26) noted that angiogenic switching was severely compromised, whereas tumor numbers

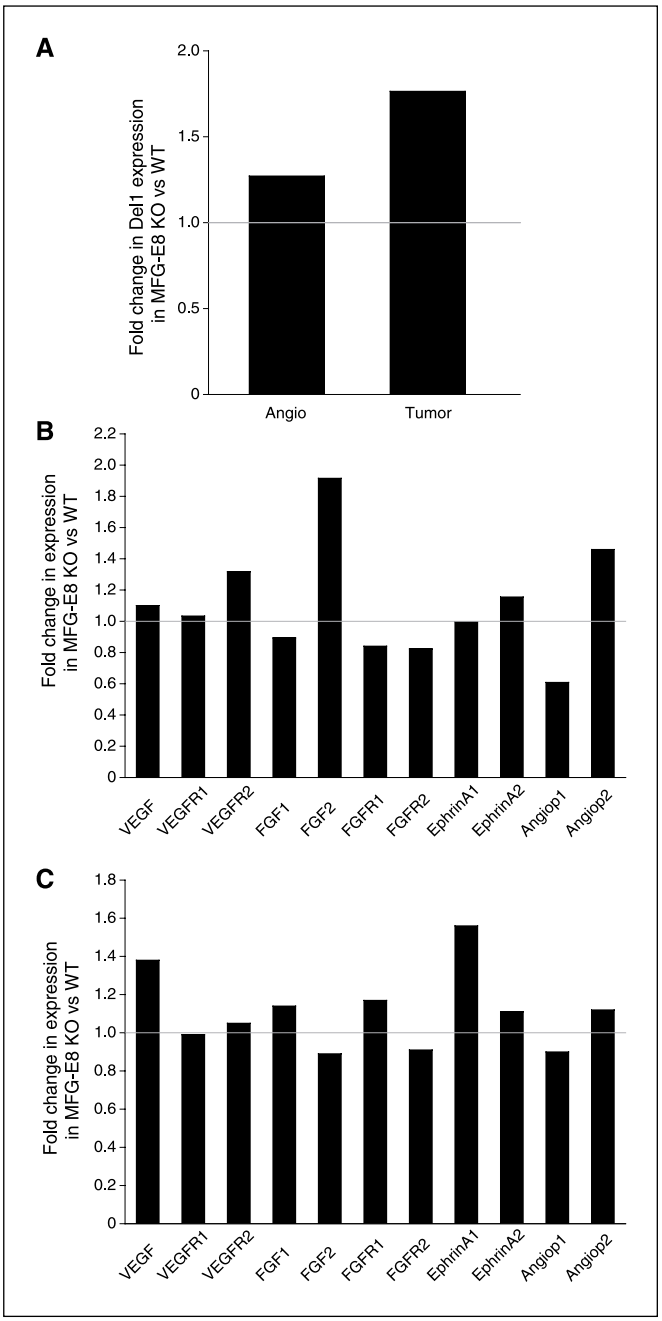

Figure 5. Compensatory increases in levels of mRNA encoding proangiogenic factors in pancreatic lesions in MFG-E8–deficient Rip1-Tag2 mice. *A,* relative levels of expression of Del1 mRNA in pooled angiogenic islets and pancreatic tumors in individual MFG-E8$^{-/-}$ and with control mice as assessed by real-time RT-PCR analysis (n = 3 mice of each genotype). Gene expression levels are expressed as fold changes in KO versus control mice normalized to glyceraldehyde-3-phosphate dehydrogenase mRNA levels in samples from individual animals. *B,* quantification of mRNAs encoding proangiogenic factors in pooled angiogenic islets from control and MFG-E8 KO animals via real-time RT-PCR (n = 3 mice of each genotype). *C,* gene expression levels of proangiogenic factors in pooled tumors from Rip1-Tag2 mice (n = 3 mice of each genotype).

were reduced by only 2-fold. If sustained, the observed ~25% difference in proliferation rates in tumor precursor lesions could result in the decreased tumor burdens that were detected in MFG-E8 KO mice, however.

We infer that MFG-E8 exerts its influence on tumorigenesis in this model primarily through potentiation of VEGF:VEGFR2 signaling to endothelial cells by engaging $\alpha_v\beta_3$ integrins as has been shown in a hind limb ischemia model (19). In this study, MFG-E8 was reported to enhance VEGF-dependent, but not FGF2-dependent, angiogenesis, an outcome ascribed in part to increased, MFG-E8–stimulated, Akt phosphorylation that may also account for our observations. In our study, we observed increased accumulation of apoptotic cells in the entire spectrum of pathologic lesions in Rip1-Tag2 MFG-E8–deficient pancreas. The distribution of apoptotic cells within pancreatic lesions did not suggest that enhanced apoptosis was restricted to endothelial cells, and this was confirmed by double staining with a vascular marker (data not shown). Although it is possible that apoptotic cells accumulated in pancreatic lesions in MFG-E8 KO mice solely because these mice exhibit an apoptotic cell uptake defect (18), tumor cells also express $\alpha_v\beta_3$ integrins and it is also possible that premalignant and/or tumor cells in MFG-E8–deficient mice undergo apoptosis more rapidly because they are not receiving MFG-E8–dependent and $\alpha_v\beta_3$-dependent prosurvival signals. Enhanced expression of Del1 in pancreatic tumors in MFG-E8 KO mice (see Fig. 5*A*) might have attenuated accumulation of apoptotic cells in tumors by increasing uptake by phagocytes or by providing a compensatory survival signal.

Engagement of $\alpha_v\beta_3$ by the MFG-E8 homologue Del1 has been reported to enhance migration of endothelial cells (12) and it is likely that MFG-E8 has comparable activity in this regard. Histologic assessment of pancreatic lesions in this study revealed an overrepresentation of adenomas and an underrepresentation of invasive carcinomas in Rip1-Tag2 MFG-E8 KO mice relative to controls, consistent with delayed tumor progression. Attenuated migratory capacity of tumor cells in MFG-E8–deficient mice could contribute to, or be responsible for, the reduction in frequency of invasive lesions that was observed.

Quantification of levels of expression of mRNA encoding a variety of regulators of angiogenesis in pancreatic lesions revealed increased expression of Del1 in tumors, and to a lesser extent in angiogenic islets, from MFG-E8–deficient mice. Increased levels of mRNA encoding VEGFR2, FGF2, and angiopoietin 2 were also detected in angiogenic islets, whereas increased levels of VEGF and EphrinA2 mRNAs were also detected in tumors. The magnitudes of these changes were not dramatic and only a small number of animals were studied. However, up-regulation of Del1 and other alternative proangiogenic regulators in MFG-E8–deficient mice may reflect induction of compensatory mechanisms that lead to an attenuated vascular phenotype. This result is consistent with recent reports documenting compensatory proangiogenic responses in tumors in animals that were treated chronically with pharmacologic agents that inhibit VEGFR2 signaling and that are responsible for emergence of resistance to antiangiogenic therapy (9). These observations suggest that effective inhibition of tumor-associated angiogenesis will require targeting of multiple complementary proangiogenic pathways as already proposed by others (9). The observation that different proangiogenic influences are increased in MFG-E8–deficient mice in precursor lesions (angiogenic islets) compared with tumors is potentially quite interesting. If confirmed for other progressing tumors, this suggests that different therapeutic agents, or combinations of agents, may be required to inhibit tumorigenesis in preventative compared with therapeutic studies. Indeed, studies by Bergers et al. (24) in the Rip1-Tag2 model suggest that this may be the case.

The recognition that tumors "escape" from antiangiogenic effects of single agents that are administered chronically as a component of cancer therapy regimens has prompted searches for new targets in proangiogenic pathways and new agents that inhibit these targets. The results reported herein support the addition of MFG-E8 to the list of relevant proangiogenic targets. As a secreted protein, MFG-E8 could potentially be targeted by appropriate mAbs. MFG-E8:$\alpha_v\beta_3$ integrin interactions could conceivably be targeted by small-molecule inhibitors. The multidomain structure of MFG-E8 may allow production of truncated proteins that are stable and that could be used as therapeutic agents. This latter approach does not differ in principal from the use of synthetic RGD-containing peptides or peptides selected from recombinant combinatorial libraries based on their ability to bind to $\alpha_v\beta_3$. However, truncated forms of MFG-E8 (such as the entire NH_2 terminus) may bind to $\alpha_v\beta_3$ with higher affinity than RGD-containing peptides that have little secondary structure and thus be more effective inhibitors. Additionally, it is likely that MFG-E8 fragments will also inhibit Del1:$\alpha_v\beta_3$ interactions, blocking at least one of the compensatory pathways that are apparently up-regulated in MFG-E8$^{-/-}$ tumors. Finally, truncated MFG-E8 species are unlikely to be antigenic. Development of MFG-E8–based therapeutics that inhibit tumor growth in the Rip1-Tag 2 and other tumor models and definition of the mechanisms by which they act will be the focus of future studies.

Acknowledgments

Received 1/12/2007; revised 3/30/2007; accepted 5/10/2007.

Grant support: Intramural Program of the NIH, Center for Cancer Research, NCI.

The costs of publication of this article were defrayed in part by the payment of page charges. This article must therefore be hereby marked *advertisement* in accordance with 18 U.S.C. Section 1734 solely to indicate this fact.

We thank Michael Lu for excellent technical assistance, Oksana Gavrilova (National Institutes of Diabetes, Digestive and Kidney Diseases/NIH, Bethesda, MD) for technical instructions, and David E. Kleiner (NCI/NIH) for evaluating histologic samples.

References

1. Hanahan D, Weinberg RA. The hallmarks of cancer. Cell 2000;100:57–70.
2. Carmeliet P, Jain RK. Angiogenesis in cancer and other diseases. Nature 2000;407:249–57.
3. Eliceiri BP. Integrin and growth factor receptor crosstalk. Circ Res 2001;89:1104–10.
4. Giancotti FG, Ruoslahti E. Integrin signaling. Science 1999;285:1028–32.
5. Guo W, Giancotti FG. Integrin signalling during tumour progression. Nat Rev Mol Cell Biol 2004;5:816–26.
6. Borges E, Jan Y, Ruoslahti E. Platelet-derived growth factor receptor β and vascular endothelial growth factor receptor 2 bind to the β_3 integrin through its extracellular domain. J Biol Chem 2000;275:39867–73.
7. Hood JD, Frausto R, Kiosses WB, Schwartz MA, Cheresh DA. Differential α_v integrin-mediated Ras-ERK signaling during two pathways of angiogenesis. J Cell Biol 2003;162:933–43.
8. Mahabeleshwar GH, Feng W, Phillips DR, Byzova TV. Integrin signaling is critical for pathological angiogenesis. J Exp Med 2006;203:2495–507.
9. Casanovas O, Hicklin DJ, Bergers G, Hanahan D. Drug resistance by evasion of antiangiogenic targeting of VEGF signaling in late-stage pancreatic islet tumors. Cancer Cell 2005;8:299–309.
10. Hidai C, Zupancic T, Penta K, et al. Cloning and

characterization of developmental endothelial locus-1: an embryonic endothelial cell protein that binds the $\alpha_v\beta_3$ integrin receptor. Genes Dev 1998;12:21–33.
11. Hanayama R, Tanaka M, Miwa K, Nagata S. Expression of developmental endothelial locus-1 in a subset of macrophages for engulfment of apoptotic cells. J Immunol 2004;172:3876–82.
12. Penta K, Varner JA, Liaw L, Hidai C, Schatzman R, Quertermous T. Del1 induces integrin signaling and angiogenesis by ligation of $\alpha_v\beta_3$. J Biol Chem 1999;274:11101–9.
13. Aoka Y, Johnson FL, Penta K, et al. The embryonic angiogenic factor Del1 accelerates tumor growth by enhancing vascular formation. Microvasc Res 2002;64:148–61.
14. Zhong J, Eliceiri B, Stupack D, et al. Neovascularization of ischemic tissues by gene delivery of the extracellular matrix protein Del-1. J Clin Invest 2003;112:30–41.
15. Stubbs JD, Lekutis C, Singer KL, et al. cDNA cloning of a mouse mammary epithelial cell surface protein reveals the existence of epidermal growth factor-like domains linked to factor VIII-like sequences. Proc Natl Acad Sci U S A 1990;87:8417–21.
16. Borisenko GG, Iverson SL, Ahlberg S, Kagan VE, Fadeel B. Milk fat globule epidermal growth factor 8 (MFG-E8) binds to oxidized phosphatidylserine: implications for macrophage clearance of apoptotic cells. Cell Death Differ 2004;11:943–5.
17. Hanayama R, Tanaka M, Miwa K, Shinohara A, Iwamatsu A, Nagata S. Identification of a factor that links apoptotic cells to phagocytes. Nature 2002;417:182–7.
18. Hanayama R, Tanaka M, Miyasaka K, et al. Autoimmune disease and impaired uptake of apoptotic cells in MFG-E8-deficient mice. Science 2004;304:1147–50.
19. Silvestre JS, Thery C, Hamard G, et al. Lactadherin promotes VEGF-dependent neovascularization. Nat Med 2005;11:499–506.
20. Hanahan D. Heritable formation of pancreatic β-cell tumours in transgenic mice expressing recombinant insulin/simian virus 40 oncogenes. Nature 1985;315:115–22.
21. Folkman J, Watson K, Ingber D, Hanahan D. Induction of angiogenesis during the transition from hyperplasia to neoplasia. Nature 1989;339:58–61.
22. Bergers G, Hanahan D, Coussens LM. Angiogenesis and apoptosis are cellular parameters of neoplastic progression in transgenic mouse models of tumorigenesis. Int J Dev Biol 1998;42:995–1002.
23. Bergers G, Brekken R, McMahon G, et al. Matrix metalloproteinase-9 triggers the angiogenic switch during carcinogenesis. Nat Cell Biol 2000;2:737–44.
24. Bergers G, Song S, Meyer-Morse N, Bergsland E, Hanahan D. Benefits of targeting both pericytes and endothelial cells in the tumor vasculature with kinase inhibitors. J Clin Invest 2003;111:1287–95.
25. Bergers G, Javaherian K, Lo KM, Folkman J, Hanahan D. Effects of angiogenesis inhibitors on multistage carcinogenesis in mice. Science 1999;284:808–12.
26. Inoue M, Hager JH, Ferrara N, Gerber HP, Hanahan D. VEGF-A has a critical, nonredundant role in angiogenic switching and pancreatic β cell carcinogenesis. Cancer Cell 2002;1:193–202.
27. Gannon G, Mandriota SJ, Cui L, Baetens D, Pepper MS, Christofori G. Overexpression of vascular endothelial growth factor-A165 enhances tumor angiogenesis but not metastasis during β-cell carcinogenesis. Cancer Res 2002;62:603–8.
28. Efrat S, Linde S, Kofod H, et al. β-Cell lines derived from transgenic mice expressing a hybrid insulin gene-oncogene. Proc Natl Acad Sci U S A 1988;85:9037–41.
29. Parangi S, O'Reilly M, Christofori G, et al. Antiangiogenic therapy of transgenic mice impairs *de novo* tumor growth. Proc Natl Acad Sci U S A 1996;93:2002–7.
30. Miles AA, Miles EM. Vascular reactions to histamine, histamine-liberator and leukotaxine in the skin of guinea-pigs. J Physiol 1952;118:228–57.
31. Ensslin MA, Shur BD. Identification of mouse sperm SED1, a bimotif EGF repeat and discoidin-domain protein involved in sperm-egg binding. Cell 2003;114:405–17.
32. Lopez T, Hanahan D. Elevated levels of IGF-1 receptor convey invasive and metastatic capability in a mouse model of pancreatic islet tumorigenesis. Cancer Cell 2002;1:339–53.